Contribution from the Department of Chemistry and Laboratory for Molecular Structure and Bonding, Texas A&M University, College Station, Texas 77843

Structures of $Mo_2(CH_3)_4(PR_3)_4$ Molecules: Constancy of Covalent Radius of Molybdenum in These and Other $Mo_2X_4(PR_3)_4$ Molecules

F. Albert Cotton* and Kenneth J. Wiesinger

Received November 3, 1989

The crystal and molecular structures of authentic, pure samples of $Mo_2Cl_3(CH_2C_6H_5)(PMe_3)_4$ (**1**), $Mo_2(CH_3)_4(PMe_3)_4$ (**2**), and $Mo_2(CH_3)_4(PMe_2Ph)_4$ (**3**) are reported. Special care was exercised in the preparation of **2** and **3** to exclude chloride and thus obviate the presence of chloride-containing contaminants. A previously reported structure for what was thought to be **2** is thus shown to be invalid owing to serious contamination by Cl^--containing impurities. The Mo–C distances in **1** and **2** are then compared to those in other $Mo_2X_4(PR_3)_4$ compounds, and it is shown that the molybdenum atom in such compounds displays an essentially constant covalent radius of 1.40 ± 0.02 Å. Crystal data for **1**–**3** are as follows. **1**: space group $P2_1/c$ with $a = 14.319$ (5) Å, $b = 10.612$ (1) Å, $c = 21.004$ (5) Å, $\beta = 106.62$ (6)°, $V = 3058$ (4) Å^3, and $Z = 4$. **2**: space group $C2/c$ with $a = 18.464$ (4) Å, $b = 9.453$ (2) Å, $c = 17.477$ (4) Å, $\beta = 116.33$ (1)°, $V = 2734$ (2) Å^3, and $Z = 4$. **3**: space group $P2/c$ with $a = 18.478$ (4) Å, $b = 11.820$ (2) Å, $c = 18.567$ (8) Å, $\beta = 109.89$ (2)°, $V = 3813$ (4) Å^3, and $Z = 4$. For **1**, the Mo–Mo, Mo–C, average Mo–Cl, and Mo–P distances are 2.1382 (3), 2.248 (3), 2.431 [2], and 2.56 [1] Å. The average Mo–Mo, Mo–C, and Mo–P distances in **2** and **3**, respectively, are 2.1489 (4) and 2.164 [1] Å, 2.244 [4] and 2.242 [8] Å, and 2.504 [1] and 2.534 [2] Å.

Introduction

Over a period of years the preparation, structural characterization, and study of other properties of numerous compounds of general formula $Mo_2X_4(PR_3)_4$ have been reported. A summary of those for which structures are available is presented in Table I.[1-5] As one can clearly see, the molybdenum covalent radius is fairly constant at 1.40 ± 0.02 Å. Taking the carbon covalent radius as 0.77 Å, a Mo–C bond distance would be predicted to be 2.17 Å. This appears to be a reasonable estimate in light of the known Mo–C bond distances in compounds containing a dinuclear Mo_2^{4+} core. Compounds of the type $Mo_2(O_2CCH_3)_2R_2(PMe_3)_2$ where R = CH_2SiMe_3 and p-$MeC_6H_5CH_2$ have been synthesized[6,7] and exhibit Mo–C bond distances of 2.231 (2) and 2.23 [1] Å, respectively. $Li_4Mo_2Me_8 \cdot 4thf$ was determined[8] to have a Mo–C bond distance of 2.29 [1] Å. These and other structural studies of similar complexes are summarized in Table II.[6-9]

The Mo–C bond distance in $Mo_2(CH_3)_4(PMe_3)_4$, the only structurally characterized $Mo_2X_4(PR_3)_4$ compound with a Mo–C bond, was reported to be 2.439 [5] Å.[9] This distance appears to be unreasonably long and prompted us to reinvestigate this system. Andersen's synthesis[9] involved the action of CH_3MgCl on an ether suspension of $Mo_2(O_2CCH_3)_4$ in the presence of excess trimethylphosphine. The results of our research indicate that the reported $Mo_2(CH_3)_4(PMe_3)_4$ compound was indeed a mixture of $Mo_2Cl_4(PMe_3)_4$ and $Mo_2(CH_3)_4(PMe_3)_4$, a Grignard reagent may act as both an alkylating and a halogenating agent, and a dialkylmagnesium reagent prepared from dialkylmercury must be used in order to eliminate all chloride-containing products.

Experimental Section

All experiments were performed under an atmosphere of dry oxygen-free argon by using standard Schlenk techniques. All solvents were freshly distilled over sodium–potassium/benzophenone under nitrogen immediately prior to use. NMR spectra were recorded on a Varian XL-200E spectrometer at 200 MHz for ^1H and 50 MHz for ^{13}C. Reference standards were C_6D_6 (7.15 ppm) for ^1H and C_6D_6 (128.228 ppm) for ^{13}C. UV–vis spectra were recorded on a Cary 17-D spectrophotometer. Trimethylphosphine and dimethylphenylphosphine were purchased from Strem Inc. and used without further purification. Dimethylmagnesium was prepared from the reaction of Mg metal with dimethylmercury (Alfa) as a diethyl ether solution, and its molarity was determined by the method of Bergbreiter;[10] yields were typically >95%.

Table I. The Molybdenum Radius (Å) As Calculated from the Structural Data for $Mo_2X_4(PR_3)_4$ Complexes

compd	Mo–Mo, Å	Mo–X, Å	Mo–P, Å	Mo radius, Å	ref
$Mo_2Cl_4(PMe_2Ph)_4$	2.1288 (8)[a]	2.418 [1]	2.549 [8]	1.43	1
$Mo_2Cl_4(PHPh_2)_4$	2.1474 (9)	2.394 [7]	2.547 [9]	1.40	1
$Mo_2Cl_4(PMe_3)_4$	2.130 (0)	2.414 [1]	2.545 [1]	1.42	2
$Mo_2(NCO)_4(PMe_3)_4$	2.134 (1)	2.072 [9]	2.53 [1]	1.37	3
$Mo_2(NCS)_4(PMe_3)_4$	2.134 (1)	2.080 [6]	2.540 [4]	1.38	3
$Mo_2I_4(PMe_3)_4$	2.129 (1)	2.759 [3]	2.562 [5]	1.43	4
$Mo_2Br_4(PMe_3)_4$	2.125 (1)	2.549 [2]	2.546 [6]	1.41	5

[a] ( ) denotes esd; [ ] denotes mean deviation from arithmetic mean of several values. [b] Taking radii (Å) of ligands as follows: Cl, 0.99; Br, 1.14; I, 1.33; N, 0.70.

Synthesis of Reported Compounds. Preparation of $Mo_2Cl_3(CH_2C_6H_5)(PMe_3)_4$. Dimolybdenum tetraacetate (0.500 g, 1.17 mmol) was partially dissolved in tetrahydrofuran (40 mL), and the mixture was cooled to −78 °C. Trimethylphosphine (0.50 mL, 4.92 mmol) and then benzylmagnesium chloride (2.34 mL, 2.0 M thf solution, 4.68 mmol) were added to the stirring solution with formation of a purple color. The solution was stirred at −78 °C for 2 h with no change in color. The cooling bath was removed, and the solution was stirred at room temperature for 10 h. All volatiles were removed via vacuum distillation; the residue was extracted with hexanes (35 mL), and the extract was filtered and reduced to 10 mL. This solution was deep purple, but after it was allowed to stand for 2 days, a fine black solid precipitated, leaving a clear light purple solution. The solution was filtered and cooled to 0 °C, which resulted in several large purple crystals. The yield was <30 mg, and the reaction has not been repeated successfully. UV–vis: 584, 443 nm (recorded as a hexane solution). ^1H NMR (C_6D_6, 298 K), δ: 6.73–7.10 ppm (m, 5 H, $-C_6H_5$); 3.26 ppm (m, 2 H, $-CH_2Ph$); 1.53 (t), 1.42 (t), 1.35 (t) ppm (virtual couplng, 9:9:18 H, $P(CH_3)_3$, $J = 4$ Hz).

$Mo_2(CH_3)_4(PMe_3)_4$. Dimolybdenum tetraacetate (0.200 g, 0.467 mmol) was suspended in diethyl ether (20 mL), and the suspension was cooled to −78 °C. Trimethylphosphine (0.30 mL, 2.95 mmol) and then dimethylmagnesium (4.87 mL, 0.43 M diethyl ether solution, 2.09 mmol) were added to the stirring solution, causing an immediate color change to deep blue. The cooling bath was removed, and the solution was stirred for 12 h. All volatiles were removed via vacuum distillation; the residue was extracted with hexanes (25 mL), and the extract was filtered and reduced to 3 mL. This solution was deep blue, which upon cooling to 0 °C gave a large batch of well-formed crystals. The yield of the reaction is near 70% and is limited only by the great solubility of the compound

---

(1) Cotton, F. A.; Daniels, L. M.; Powell, G. L. *Inorg. Chim. Acta* **1988**, *144*, 109.

(2) Cotton, F. A.; Extine, M. W.; Felthouse, T. R.; Kolthammer, B. W. S.; Lay, D. G. *J. Am. Chem. Soc.* **1981**, *103*, 4040.

(3) Cotton, F. A.; Matusz, M. *Inorg. Chem.* **1988**, *27*, 2127.

(4) Cotton, F. A.; Poli, R. *Inorg. Chem.* **1987**, *26*, 3228.

(5) Hopkins, M. D.; Schaefer, W. P.; Bronikowski, M. J.; Woodruff, W. H.; Miskowski, V. M.; Dallinger, R. F.; Gray, H. B. *J. Am. Chem. Soc.* **1987**, *109*, 408.

(6) Hursthouse, M. B.; Malik, K. M. A. *Acta Crystallogr., Sect. B* **1979**, *35* (11), 2709.

(7) Beshouri, S. M.; Fanwick, P. E.; Rothwell, I. P. *Inorg. Chim. Acta* **1987**, *129*, 87.

(8) Cotton, F. A.; Troup, J. M.; Webb, T. R.; Williamson, D. H.; Wilkinson, G. *J. Am. Chem. Soc.* **1974**, *96*, 3824.

(9) Girolami, G. S.; Mainz, V. V.; Andersen, R. A.; Vollmer, S. H.; Day, V. W. *J. Am. Chem. Soc.* **1981**, *103*, 3953.

(10) Bergbreiter, D. E.; Pendergrass, E. *J. Org. Chem.* **1981**, *46*, 219.

0020-1669/90/1329-2594$02.50/0

Table II. Structural Parameters for Alkyl-Containing Mo_2^{4+} Core Compounds

compd	Mo–Mo, Å	Mo–C, Å	Mo–P, Å	Mo radius, Å[b]	ref
$Mo_2(O_2CCH_3)_2(CH_2SiMe_3)_2(PMe_3)_2$	2.0984 (5)[a]	2.231 (2)	2.547 (1)	1.46	6
$Mo_2(O_2CCH_3)_2(p\text{-}MeC_6H_5CH_2)_2(PMe_3)_2$	2.108 [1]	2.23 [1]	2.529 [8]	1.46	7
$Li_4Mo_2Me_8\cdot4thf$	2.148 (2)	2.29 [1]		1.52	8
$Mo_2Cl_3(CH_2C_6H_5)(PMe_3)_4$	2.1382 (3)	2.248 (3)	2.56 [1]	1.48	this work
$Mo_2Me_4(PMe_3)_4$	2.1489 (4)	2.244 [4]	2.504 [1]	1.47	this work
$Mo_2Me_4(PMe_2Ph)_4$	2.164 [1]	2.242 [8]	2.534 [2]	1.47	this work
$Mo_2Me_4(PMe_3)_4$	2.153 (1)	2.439 [5]	2.513 [5]	1.67	9

[a] ( ) denotes esd; [ ] denotes mean deviation from arithmetic mean of several values. [b] Taking the radius of carbons as 0.77 Å.

Table III. Crystal Data for $Mo_2Cl_3(CH_2C_6H_5)(PMe_3)_4$, $Mo_2Me_4(PMe_3)_4$, and $Mo_2Me_4(PMe_2Ph)_4$

	1	**2**	**3**
formula	$Mo_2P_4Cl_3C_{19}H_{43}$	$Mo_2P_4C_{16}H_{48}$	$Mo_2P_4C_{36}H_{56}$
fw	693.69	556.34	804.62
space group	$P2_1/c$	$C2/c$	$P2/c$
a, Å	14.319 (5)	18.464 (4)	18.478 (4)
b, Å	10.612 (1)	9.453 (2)	11.820 (2)
c, Å	21.004 (5)	17.477 (4)	18.567 (8)
β, deg	106.62 (6)	116.33 (1)	109.89 (2)
V, Å^3	3058 (4)	2734 (2)	3813 (4)
Z	4	4	4
d_{calc}, g/cm^3	1.506	1.352	1.401
cryst size, mm	0.70 × 0.46 × 0.21	0.69 × 0.41 × 0.41	0.26 × 0.25 × 0.19
μ(Mo Kα), cm^{-1}	12.79	11.26	8.30
data collcn instrument	Enraf-Nonius CAD-4	P3	AFC-5R
radiation monochromated in incident beam: λ(Mo Kα), Å	0.71073	0.71073	0.71073
orientation reflns: no., range, deg	25; $23 < 2\theta \leq 33$	25; $19 < 2\theta \leq 30$	24; $22 < 2\theta \leq 30$
T, °C	−40	23	22
scan method	ω–2θ	ω–2θ	ω–2θ
data collcn range, deg	$4 \leq 2\theta \leq 45$	$4 \leq 2\theta \leq 50$	$4 \leq 2\theta \leq 50$
no. of unique data, total with $F_o^2 > 3\sigma(F_o^2)$	3990, 3489	2324, 2149	5873, 4580
no. of params refined	383	175	554
transm factors: max, min	1.00, 0.93	1.00, 0.92	1.00, 0.92
R[a]	0.0212	0.0281	0.0317
R_w[b]	0.0330	0.0413	0.0507
quality-of-fit indicator[c]	1.079	1.114	1.472
largest shift/esd, final cycle	0.04	0.53	0.59
largest peak, e/Å^3	0.323	0.232	0.566

[a] $R = \sum||F_o| - |F_c||/\sum|F_o|$. [b] $R_w = [\sum w(|F_o| - |F_c|)^2/\sum w|F_o|^2]^{1/2}$; $w = 1/\sigma^2(|F_o|)$. [c] Quality-of-fit $= [\sum w(|F_o| - |F_c|)^2/(N_{observns} - N_{params})]^{1/2}$.

Table IV. Positional Parameters and Equivalent Isotropic Thermal Parameters (Å^2) and Their Estimated Standard Deviations for $Mo_2Cl_3(CH_2C_6H_5)(PMe_3)_4$ (**1**)

atom	x	y	z	B[a]
Mo(1)	0.30522 (2)	0.17618 (2)	0.16448 (1)	2.591 (5)
Mo(2)	0.16160 (2)	0.24484 (2)	0.15539 (1)	2.649 (5)
Cl(1)	0.32733 (6)	−0.04751 (7)	0.19197 (4)	4.32 (2)
Cl(2)	0.14204 (5)	0.31841 (7)	0.26027 (4)	4.01 (2)
Cl(3)	0.05165 (6)	0.22714 (8)	0.04412 (4)	4.29 (2)
P(1)	0.28394 (6)	0.09972 (8)	0.04515 (4)	3.65 (2)
P(2)	0.38152 (5)	0.21044 (8)	0.29002 (4)	3.17 (2)
P(3)	0.07401 (6)	0.05069 (7)	0.17992 (4)	3.55 (2)
P(4)	0.16357 (6)	0.47830 (7)	0.12665 (4)	3.68 (2)
C(1)	0.2022 (2)	−0.0327 (3)	0.0181 (2)	5.12 (8)
C(2)	0.2479 (3)	0.2062 (4)	−0.0256 (2)	5.66 (9)
C(3)	0.3972 (2)	0.0329 (4)	0.0368 (2)	5.21 (8)
C(4)	0.3362 (2)	0.1154 (4)	0.3464 (2)	4.61 (8)
C(5)	0.5089 (2)	0.1624 (4)	0.3139 (2)	4.63 (8)
C(6)	0.3909 (2)	0.3671 (3)	0.3262 (2)	4.78 (8)
C(7)	0.1133 (2)	−0.0263 (3)	0.2597 (2)	5.19 (8)
C(8)	0.0485 (3)	−0.0830 (3)	0.1235 (2)	5.42 (9)
C(9)	−0.0479 (2)	0.1046 (4)	0.1757 (2)	5.23 (9)
C(10)	0.2365 (3)	0.5861 (3)	0.1883 (2)	5.53 (9)
C(11)	0.0399 (3)	0.5369 (3)	0.1165 (2)	5.44 (9)
C(12)	0.1855 (3)	0.5306 (4)	0.0496 (2)	6.3 (1)
C(13)	0.3998 (2)	0.3377 (3)	0.1517 (2)	4.14 (7)
C(14)	0.4803 (2)	0.3119 (3)	0.1207 (2)	3.71 (7)
C(15)	0.5635 (3)	0.2440 (3)	0.1542 (2)	4.82 (8)
C(16)	0.6385 (3)	0.2244 (4)	0.1268 (2)	5.9 (1)
C(17)	0.6353 (3)	0.2703 (4)	0.0660 (2)	5.91 (9)
C(18)	0.5547 (3)	0.3355 (4)	0.0319 (2)	6.1 (1)
C(19)	0.4783 (2)	0.3572 (3)	0.0585 (2)	4.70 (8)

[a] Anisotropically refined atoms are given in the form of the equivalent isotropic displacement parameter defined as $(4/3)[a^2\beta_{11} + b^2\beta_{22} + c^2\beta_{33} + ab(\cos\gamma)\beta_{12} + ac(\cos\beta)\beta_{13} + bc(\cos\alpha)\beta_{23}]$.

in all typical solvents. UV–vis: 590, 484, 333 nm (recorded as a hexane solution). ^{1}H NMR (C_6D_6, 298 K), δ: 1.264 ppm (t, virtual coupling, 36 H, $P(CH_3)_3$, J = 3 Hz); −0.482 ppm (t, 12 H, Mo–CH_3, J = 7 Hz). ^{13}C NMR (C_6D_6, 298 K), δ: 15.865 ppm (m, 12 C, $P(CH_3)_3$, J = 4 Hz); 2.140 ppm (t, 4 C, Mo–CH_3, J = 9 Hz).

$Mo_2(CH_3)_4(PMe_2Ph)_4$. Dimolybdenum tetraacetate (0.200 g, 0.467 mmol) was suspended in diethyl ether (20 mL), and the suspension was cooled to 0 °C. Dimethylphenylphosphine (0.40 mL, 2.80 mmol) and then dimethylmagnesium (4.87 mL, 0.43 M diethyl ether solution, 2.09 mmol) were added to the stirring solution, causing an immediate color change to deep blue. The cooling bath was removed, and the solution was stirred for 15 h. All volatiles were removed via vacuum distillation; the residue was extracted with hexanes (25 mL), and the extract was filtered and reduced to 7 mL. This solution was deep blue and upon cooling to 0 °C gave a small batch of well-formed crystals. The yield of the reaction is near 30%. A preferable method involves extracting the residue with toluene and then layering with hexanes, which results in an 85% yield. UV–vis: 615, 490 nm (recorded as a mineral oil mull). ^{1}H NMR (C_6D_6, 298 K), δ: 7.0–7.35 ppm (m, 20 H, P–C_6H_5); 1.439 ppm (t, virtual coupling, 24 H, $P(CH_3)_2$, J = 3 Hz); −0.352 ppm (t, 12 H, Mo–CH_3, J = 7 Hz). ^{13}C NMR (C_6D_6, 298 K), δ: 13.82 ppm (m, 8 C, $P(CH_3)_2Ph$, J = 4 Hz); 4.93 ppm (t, 4 C, Mo–CH_3, J = 10 Hz).

X-ray Diffraction Experiments. In each case, slow cooling of a saturated solution of the compound in hexanes to 0 °C resulted in crystals suitable for X-ray diffraction. In all cases, the crystals were handled in degassed mineral oil (stored over sodium), cut to the proper size, coated with epoxy resin, and mounted on a glass or quartz fiber. The relevant crystallographic information is given in Table III. The X-ray data were collected and corrected as described elsewhere.[11] Periodic collection of three intensity standards showed no significant (<5%) decay for any of the reported crystal structures.

The systematic absences in the data set for **1** uniquely defined its space group as $P2_1/c$. A three-dimensional Patterson function suggested a dimolybdenum core bonded to four phosphorus atoms and four chloride atoms. The atoms were entered and brought to convergence (R = 12) in a full-matrix isotropic least-squares refinement. One "chloride" atom had an istropic thermal parameter of 22 Å^2. A difference Fourier map revealed that this "chloride" atom was in fact a carbon atom in a benzyl ligand. All carbon atoms were found and entered; this model was refined to isotropic convergence. After anisotropic refinement to R = 3.7, a difference Fourier map revealed all hydrogen atoms. These were entered and refined without constraints. Eleven hydrogen atoms were not behaving properly with regard to their thermal and/or positional parameters. Therefore, all hydrogen thermal parameters were constrained to that of H(1). This model was refined successfully to convergence; the final figures of merit are listed in Table III. The final non-hydrogen fractional atomic coordinates and the selected bond distances and angles are listed in Tables IV and V, respectively.

For **2**, the possible space groups were Cc and $C2/c$. Since Cc is a subgroup of $C2/c$, refinement was started in this space group. A three-dimensional Patterson function revealed a dimolybdenum core bonded to four phosphorus atoms. After several full-matrix isotropic least-squares refinements, it was apparent that a 2-fold proper rotation

---

(11) Bino, A.; Cotton, F. A.; Fanwick, P. E. *Inorg. Chem.* **1979**, *18*, 3558.

Table V. Selected Bond Distances (Å) and Bond Angles (deg) for $Mo_2Cl_3(CH_2C_6H_5)(PMe_3)_4$ (**1**)[a]

	Distances		
Mo(1)–Mo(2)	2.1382 (3)	Mo(2)–Cl(2)	2.428 (1)
Mo(1)–Cl(1)	2.442 (1)	Mo(2)–Cl(3)	2.423 (1)
Mo(1)–P(1)	2.568 (1)	Mo(2)–P(3)	2.540 (1)
Mo(1)–P(2)	2.575 (1)	Mo(2)–P(4)	2.552 (1)
Mo(1)–C(13)	2.248 (3)	C(13)–C(14)	1.503 (5)
	Angles		
Mo(2)–Mo(1)–Cl(1)	114.12 (2)	Mo(1)–Mo(2)–Cl(3)	113.75 (3)
Mo(2)–Mo(1)–P(1)	100.25 (2)	Mo(1)–Mo(2)–P(3)	102.92 (2)
Mo(2)–Mo(1)–P(2)	99.14 (2)	Mo(1)–Mo(2)–P(4)	106.05 (2)
Mo(2)–Mo(1)–C(13)	109.05 (8)	Cl(2)–Mo(2)–Cl(3)	133.50 (3)
Cl(1)–Mo(1)–P(1)	83.96 (3)	Cl(2)–Mo(2)–P(3)	83.40 (3)
Cl(1)–Mo(1)–P(2)	84.65 (3)	Cl(2)–Mo(2)–P(4)	85.09 (3)
Cl(1)–Mo(1)–C(13)	136.70 (8)	Cl(3)–Mo(2)–P(3)	84.86 (3)
P(1)–Mo(1)–P(2)	160.23 (3)	Cl(3)–Mo(2)–P(4)	83.98 (3)
P(1)–Mo(1)–C(13)	91.83 (9)	P(3)–Mo(2)–P(4)	151.02 (3)
P(2)–Mo(1)–C(13)	85.45 (8)	Mo(1)–C(13)–C(14)	118.4 (2)
Mo(1)–Mo(2)–Cl(2)	112.72 (2)		

[a] Numbers in parentheses are estimated standard deviations in the least significant digits.

Table VI. Positional Parameters and Equivalent Isotropic Thermal Parameters (Å^2) and Their Estimated Standard Deviations for $Mo_2Me_4(PMe_3)_4$ (**2**)

atom	x	y	z	B[a]
Mo(1)	0.000	0.08742 (3)	0.250	2.549 (9)
Mo(2)	0.000	0.31474 (3)	0.250	2.65 (1)
P(1)	0.11828 (4)	0.03160 (8)	0.38952 (5)	3.66 (2)
P(2)	0.08998 (5)	0.37036 (9)	0.18101 (5)	4.07 (2)
C(1)	−0.0739 (2)	−0.0122 (4)	0.3089 (2)	4.45 (7)
C(2)	0.0975 (2)	0.4146 (3)	0.3664 (2)	4.44 (7)
C(11)	0.2202 (2)	0.0834 (4)	0.4087 (2)	5.45 (8)
C(12)	0.1198 (3)	0.0779 (5)	0.4909 (2)	6.11 (8)
C(13)	0.1293 (3)	−0.1606 (4)	0.4005 (3)	7.0 (1)
C(21)	0.1960 (3)	0.3155 (5)	0.2302 (4)	7.6 (1)
C(22)	0.0994 (3)	0.5612 (4)	0.1763 (3)	6.36 (9)
C(23)	0.0592 (3)	0.3246 (5)	0.0690 (3)	6.7 (1)

[a] Anisotropically refined atoms are given in the form of the equivalent isotropic displacement parameter defined as $(4/3)[a^2\beta_{11} + b^2\beta_{22} + c^2\beta_{33} + ab(\cos\gamma)\beta_{12} + ac(\cos\beta)\beta_{13} + bc(\cos\alpha)\beta_{23}]$.

Table VII. Selected Bond Distances (Å) and Bond Angles (deg) for $Mo_2Me_4(PMe_3)_4$ (**2**)[a]

	Distances		
Mo(1)–Mo(2)	2.1489 (4)	Mo(2)–P(2)	2.503 (1)
Mo(1)–P(1)	2.504 (1)	Mo(2)–C(2)	2.241 (3)
Mo(1)–C(1)	2.248 (4)		
	Angles		
Mo(2)–Mo(1)–P(1)	102.17 (2)	Mo(1)–Mo(2)–P(2)	102.12 (2)
Mo(2)–Mo(1)–C(1)	114.77 (9)	Mo(1)–Mo(2)–C(2)	114.93 (8)
P(1)–Mo(1)–P(1)′	155.67 (3)	P(2)–Mo(2)–P(2)′	155.75 (3)
P(1)–Mo(1)–C(1)	84.85 (7)	P(2)–Mo(2)–C(2)	84.9 (1)
P(1)–Mo(1)–C(1)′	85.02 (7)	P(2)–Mo(2)–C(2)′	85.0 (1)
C(1)–Mo(1)–C(1)′	130.5 (1)	C(2)–Mo(2)–C(2)′	130.1 (1)

[a] Numbers in parentheses are estimated standard deviations in the least significant digits.

Table VIII. Positional and Thermal Parameters (Å^2) and Their Estimated Standard Deviations for $Mo_2Me_4(PMe_2Ph)_4$ (**3**)

atom	x	y	z	B[a]
Mo(1)	0.000	0.17263 (4)	0.250	2.35 (1)
Mo(2)	0.000	0.35573 (4)	0.250	2.29 (1)
P(1)	0.12390 (7)	0.1319 (1)	0.35898 (6)	3.01 (3)
P(2)	0.07176 (7)	0.3961 (1)	0.15835 (6)	2.79 (3)
C(1)	−0.0524 (3)	0.0912 (4)	0.3293 (3)	3.33 (7)
C(2)	−0.1058 (3)	0.4335 (3)	0.1644 (3)	3.40 (7)
C(11)	0.1419 (3)	0.1980 (4)	0.4527 (3)	4.62 (8)
C(12)	0.2176 (3)	0.1513 (4)	0.3465 (3)	4.21 (8)
C(13)	0.1315 (3)	−0.0192 (4)	0.3846 (3)	3.41 (7)
C(14)	0.1225 (3)	−0.0584 (4)	0.4520 (3)	4.26 (8)
C(15)	0.1316 (4)	−0.1721 (5)	0.4696 (3)	5.75 (8)
C(16)	0.1442 (4)	−0.2488 (5)	0.4208 (4)	5.73 (8)
C(17)	0.1505 (4)	−0.2118 (4)	0.3532 (4)	5.37 (8)
C(18)	0.1442 (3)	−0.0994 (4)	0.3354 (3)	4.31 (8)
C(21)	0.0245 (3)	0.3683 (4)	0.0569 (3)	3.83 (7)
C(22)	0.1658 (3)	0.3297 (4)	0.1760 (3)	3.86 (7)
C(23)	0.0943 (3)	0.5466 (4)	0.1553 (2)	3.06 (7)
C(24)	0.1607 (3)	0.5839 (4)	0.1439 (3	4.47 (8)
C(25)	0.1735 (3)	0.7001 (5)	0.1392 (3)	4.95 (8)
C(26)	0.1222 (3)	0.7768 (4)	0.1443 (3)	4.37 (8)
C(27)	0.0559 (3)	0.7406 (4)	0.1552 (3)	4.32 (8)
C(28)	0.0420 (3)	0.6286 (4)	0.1609 (3)	3.90 (7)
Mo(3)	0.500	0.84305 (4)	0.250	2.52 (1)
Mo(4)	0.500	1.02618 (4)	0.250	2.50 (1)
P(3)	0.56182 (7)	0.7994 (1)	0.15032 (7)	3.14 (3)
P(4)	0.62783 (7)	1.0715 (1)	0.35204 (7)	2.97 (3)
C(3)	0.3918 (3)	0.7663 (4)	0.1711 (3)	3.78 (7)
C(4)	0.4551 (3)	1.1036 (4)	0.3370 (3)	3.79 (7)
C(31)	0.5082 (3)	0.8249 (4)	0.0486 (3)	4.37 (8)
C(32)	0.6551 (3)	0.8649 (4)	0.1604 (3)	4.50 (8)
C(33)	0.5838 (3)	0.6485 (4)	0.1445 (3)	3.50 (7)
C(34)	0.5251 (3)	0.5725 (5)	0.1185 (4)	5.87 (8)
C(35)	0.5395 (4)	0.4571 (5)	0.1085 (4)	7.26 (9)
C(36)	0.6114 (4)	0.4209 (5)	0.1243 (4)	5.99 (8)
C(37)	0.6718 (4)	0.4957 (6)	0.1505 (4)	6.51 (8)
C(38)	0.6583 (3)	0.6080 (5)	0.1618 (4)	5.38 (8)
C(41)	0.6488 (3)	1.0088 (4)	0.4468 (3)	4.02 (7)
C(42)	0.7177 (3)	1.0442 (4)	0.3341 (3)	4.39 (8)
C(43)	0.6382 (3)	1.2236 (4)	0.3732 (3)	3.43 (7)
C(44)	0.6188 (4)	1.3025 (4)	0.3139 (3)	5.24 (8)
C(45)	0.6295 (4)	1.4150 (5)	0.3275 (3)	6.01 (8)
C(46)	0.6612 (3)	1.4566 (5)	0.4000 (4)	5.02 (8)
C(47)	0.6805 (4)	1.3816 (5)	0.4598 (3)	6.10 (8)
C(48)	0.6698 (4)	1.2655 (5)	0.4466 (3)	5.50 (8)

[a] Anisotropically refined atoms are given in the form of the equivalent isotropic displacement parameter defined as $(4/3)[a^2\beta_{11} + b^2\beta_{22} + c^2\beta_{33} + ab(\cos\gamma)\beta_{12} + ac(\cos\beta)\beta_{13} + bc(\cos\alpha)\beta_{23}]$.

axis existed along the Mo–Mo bond axis. The space group was changed to $C2/c$. Subsequent least-squares refinements and difference Fourier maps revealed all remaining non-hydrogen atoms. After all atoms were refined to anisotropic convergence ($R = 5.4\%$), most hydrogen atoms were found in a difference Fourier map and their positions entered. However, none of them refined properly, and they were deleted and reentered with the program HYDRO and refined in the program SHELX-76 with fixed C–H distances. Again the refinement failed. An analysis of the data was run with the program PERFACT. It was determined that 14 of the first 22 worst reflections (largest $W{\cdot}DEL^2$ values) had $\chi = 72°$ (±4°). Considering the above difficulties, it was decided to re-collect the first 22 worst reflections.[12] The structure was successfully refined in SHELX-76 with constraints put on all the C–H interatomic distances and their isotropic thermal parameters. The final figures of merit are listed in Table III. The final non-hydrogen fractional atomic coordinates and the selected bond distances and angles are listed in Tables VI and VII, respectively.

For **3**, the possible space groups were Pc and $P2/c$. Refinement was started in Pc. A three-dimensional Patterson function revealed two independent dimolybdenum cores. After a cycle of scale factor refinement, all 16 phosphorus atoms and all but 10 carbon atoms were located and entered. A 2-fold axis was found along the Mo–Mo bonds, the space group was changed to $P2/c$, and the appropriate atoms were deleted. Succesive full-matrix least-squares refinements and difference Fourier maps resulted in convergence at $R = 6.4\%$. After all atoms were refined anisotropically to convergence ($R = 4.7\%$), all hydrogen atoms were found in a difference Fourier map and their positions entered. The structure was refined with restraints put on the C–H interatomic distances and their isotropic thermal parameters. The final figures of merit are listed in Table III. The final non-hydrogen fractional atomic coordinates and the selected bond distances and angles are listed in Tables VIII and IX, respectively.

Results and Discussion

Synthetic Methods. $Mo_2Cl_3(CH_2C_6H_5)(PMe_3)_4$. In our attempt to prepare $Mo_2(CH_2C_6H_5)_4(PMe_3)_4$, we obtained compound **1**. The most interesting feature of this compound is its mixed hal-

---

(12) A crystal from another batch was used and had the dimensions 0.70 × 0.35 × 0.40 mm. The collection and reduction of data were performed in a manner similar to that for the first data set. The re-collected data set contained 260 reflections that were common to the first set. The merge factor was $R_{merge} = 0.0150$.

Table IX. Selected Bond Distances (Å) and Bond Angles (deg) for $Mo_2Me_4(PMe_2Ph)_4$ (**3**)[a]

	Distances		
Mo(1)-Mo(2)	2.164 (1)	Mo(3)-Mo(4)	2.165 (1)
Mo(1)-P(1)	2.533 (1)	Mo(3)-P(3)	2.537 (1)
Mo(1)-C(1)	2.236 (5)	Mo(3)-C(3)	2.231 (4)
Mo(2)-P(2)	2.533 (1)	Mo(4)-P(4)	2.532 (1)
Mo(2)-C(2)	2.254 (4)	Mo(4)-C(4)	2.246 (5)
	Angles		
Mo(2)-Mo(1)-P(1)	100.96 (3)	Mo(4)-Mo(3)-P(3)	101.73 (3)
Mo(2)-Mo(1)-C(1)	115.5 (1)	Mo(4)-Mo(3)-C(3)	114.0 (1)
P(1)-Mo(1)-P(1)′	158.08 (4)	P(3)-Mo(3)-P(3)′	156.54 (4)
P(1)-Mo(1)-C(1)	82.4 (1)	P(3)-Mo(3)-C(3)	87.9 (2)
P(1)-Mo(1)-C(1)′	88.2 (1)	P(3)-Mo(3)-C(3)′	82.6 (2)
C(1)-Mo(1)-C(1)′	129.0 (2)	C(3)-Mo(3)-C(3)′	132.0 (2)
Mo(1)-Mo(2)-P(2)	100.86 (3)	Mo(3)-Mo(4)-P(4)	102.22 (3)
Mo(1)-Mo(2)-C(2)	114.1 (1)	Mo(3)-Mo(4)-C(4)	114.1 (1)
P(2)-Mo(2)-P(2)′	158.28 (4)	P(4)-Mo(4)-P(4)′	155.56 (4)
P(2)-Mo(2)-C(2)	88.6 (1)	P(4)-Mo(4)-C(4)	81.6 (1)
P(2)-Mo(2)-C(2)′	82.5 (1)	P(4)-Mo(4)-C(4)′	88.5 (1)
C(2)-Mo(2)-C(2)′	131.9 (2)	C(4)-Mo(4)-C(4)′	131.9 (2)

[a] Numbers in parentheses are estimated standard deviations in the least significant digits.

ide/alkyl composition, which was unexpectedly obtained by use of a Grignard reagent. This ability for the Grignard reagent to act as either a halogenating or an alkylating agent is of great importance when isolation of pure alkyl compounds of the type $Mo_2(CH_3)_4(PR_3)_4$ is attempted, as will be shown shortly. As noted in the Experimental Section, many side reactions occur and this reaction has not been reproducible.

It was our observations on **1** that led us to become suspicious of and therefore to reinvestigate the previous work on $Mo_2(CH_3)_4(PMe_3)_4$. This compound (**1**) is slightly more sensitive to air in the solid state than the $Mo_2Cl_4(PMe_3)_4$ compound. The solubilities and UV–vis spectra are nearly identical. In the solid state, the molecule crystallizes as enantiomorphic pairs, but this is due to the crystal packing forces. This packing orients the two hydrogens of the benzyl CH_2 group in different environments. This should lead to two different peaks in the ^1H NMR spectrum. However, the CH_2 group of the benzyl ligand appears as one multiplet in the ^1H NMR spectrum at 3.62 ppm (2 H), which indicates a rapid conformational change between the two enantiomorphs. The trimethylphosphine ligands give resonances in the ^1H NMR spectrum at 1.53 (t), 1.42 (t), and 1.35 (t) ppm (virtual coupling, 9:9:18 H, $J = 4.3$ Hz), which are consistent with the trimethylphosphine ligands being in a trans configuration. The peak at 1.35 ppm is assigned to the trimethylphosphine ligands of P(1) and P(2), as shown in Figure 1. The other two peaks are assigned to those of P(3) (1.42 ppm) and P(4) (1.53 ppm). The peak at 1.42 ppm was assigned to the P(3) ligand since it has essentially the same environment as a trimethylphosphine ligand in $Mo_2Cl_4(PMe_3)_4$, which has a shift of 1.441 ppm. This leaves the peak at 1.53 ppm assigned to the P(4) ligand. When the ^1H NMR spectrum of this sample tube was reexamined about 12 h later, only signals consistent with $Mo_2Cl_4(PMe_3)_4$ and toluene were seen.

$Mo_2(CH_3)_4(PR_3)_4$. Pure $Mo_2(CH_3)_4(PR_3)_4$ compounds (PR_3 = PMe_3, PMe_2Ph) can be prepared by reacting halide-free dimethylmagnesium with dimolybdenum(II) tetraacetate in the presence of excess phosphine.

$$Mo_2(O_2CCH_3)_4 + 2.5Me_2Mg + {>}5PR_3 \rightarrow Mo_2(CH_3)_4(PR_3)_4$$

Without rigorous exclusion of halide, a mixture of products having Mo–Cl bonds as well as Mo–CH_3 bonds is obtained. For reasons now to be given, we believe that, in fact, only the tetramethyl and tetrachloro species occur in detectable amounts. The following discussion will focus on the PMe_3 derivative.

The easiest way to differentiate between $Mo_2(CH_3)_4(PMe_3)_4$ and $Mo_2Cl_4(PMe_3)_4$ species is by ^1H NMR spectroscopy. The hydrogen atoms of trimethylphosphine give shifts of 1.264 (t) and 1.441 (t) ppm in the methyl and chloro analogues, respectively. In all reactions, the ^1H NMR spectrum shows no peaks in the phosphine region other than these two, which indicates that no mixed species of the type $Mo_2Cl_{4-n}Me_4(PMe_3)_4$ (with n = 1, 2, or 3) are present. A species such as $Mo_2Cl_3Me(PMe_3)_4$ would display three distinct resonances analogous to those of the $Mo_2Cl_3(CH_2C_6H_5)(PMe_3)_4$ species mentioned above. None are present.

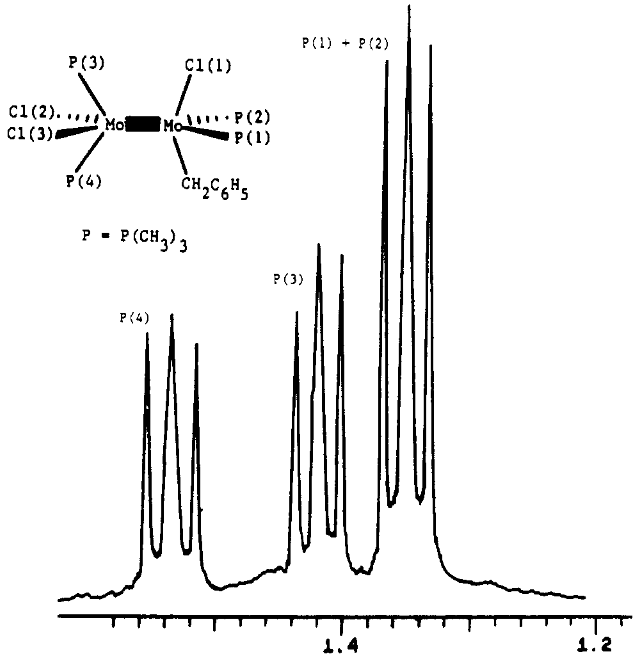

Figure 1. The trimethylphosphine region of the ^1H NMR spectrum for $Mo_2Cl_3(CH_2C_6H_5)(PMe_3)_4$ (**1**).

The crystallized products from reactions of $Mo_2Cl_4(PMe_3)_4$ with methyllithium (<6 equiv) lead to a mixture of $Mo_2Cl_4(PMe_3)_4$ and $Mo_2(CH_3)_4(PMe_3)_4$, as evidenced by ^1H NMR analysis. When >8 equiv of methylithium was used, the ^1H NMR spectrum indicated free phosphine and $Li_4Mo_2Me_8$ along with the disappearance of all peaks in the region of bound phosphine (1.1–1.5 ppm). These results prompted us to pursue the use of dimethylmagnesium.

The most common methods for the synthesis of dimethylmagnesium are the dioxane reaction (a) or the metalation reaction (b). The advantage of (a) is the ease of preparation and the

$$2CH_3MgCl + 2\,\text{dioxane} \rightarrow (CH_3)_2Mg + MgCl_2(\text{dioxane}) \quad (a)$$

$$(CH_3)_2Hg + Mg\ (\text{excess}) \rightarrow (CH_3)_2Mg + Hg/Mg \quad (b)$$

avoidance of mercury; a particular disadvantage for our system is the presence of 5–10% Cl^-. In fact, preparation of $Mo_2(CH_3)_4(PMe_3)_4$ by use of $(CH_3)_2Mg$ prepared by method a results in a mixture of $Mo_2(CH_3)_4(PMe_3)_4$ (92%) and $Mo_2Cl_4(PMe_3)_4$ (8%), as shown by the ^1H NMR spectrum in Figure 2. When $(CH_3)_2Mg$ prepared by method b is used, the pure $Mo_2(CH_3)_4(PR_3)$ compounds are obtained. The ^1H NMR spectrum is simple for pure $Mo_2(CH_3)_4(PMe_3)_4$ and contains two resonances: 1.264 (t, PMe_3) and −0.482 ppm (t, Mo–Me). The ^1H NMR spectrum for $Mo_2(CH_3)_4(PMe_2Ph)_4$ is equally simple. Further analytical details are included in the Experimental Section.

Solutions of **2** and **3** are extremely air and moisture sensitive. Very dilute solutions of **3** decompose within minutes at room temperature even in the presence of excess phosphine. This is probably due to small amounts of residual oxygen or water in the solvents. Solutions of **2** last long enough to obtain UV–visible spectra but decompose too quickly to obtain accurate values of the molar absorptivity. The solid is stable for a short period of time in air, and it apears that an oxide layer forms on the surface of crystals. Contrary to Wilkinson's report,[13] compounds **2** and

---

(13) Andersen, R. A.; Jones, R. A.; Wilkinson, G. *J. Chem. Soc., Dalton Trans.* **1978**, 446.

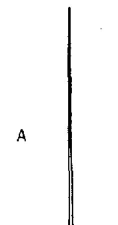

Figure 2. The trimethylphosphine region of the ^1H NMR spectrum for $Mo_2(CH_3)_4(PMe_3)_4$ prepared from chloride-contaminated $(CH_3)_2Mg$: (A) $Mo_2(CH_3)_4(PMe_3)_4$ (92%); (B) $Mo_2Cl_4(PMe_3)_4$ (8%).

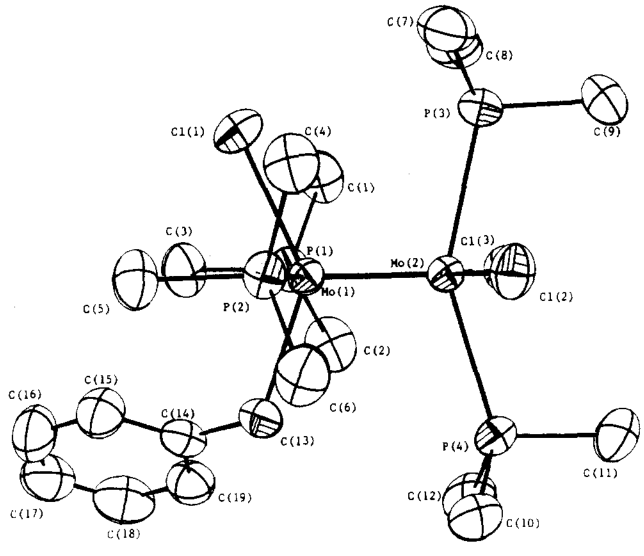

Figure 3. ORTEP drawing of the $Mo_2Cl_3(CH_2C_6H_5)(PMe_3)_4$ (**1**) molecule. Atoms are represented by their ellipsoids at the 50% probability level.

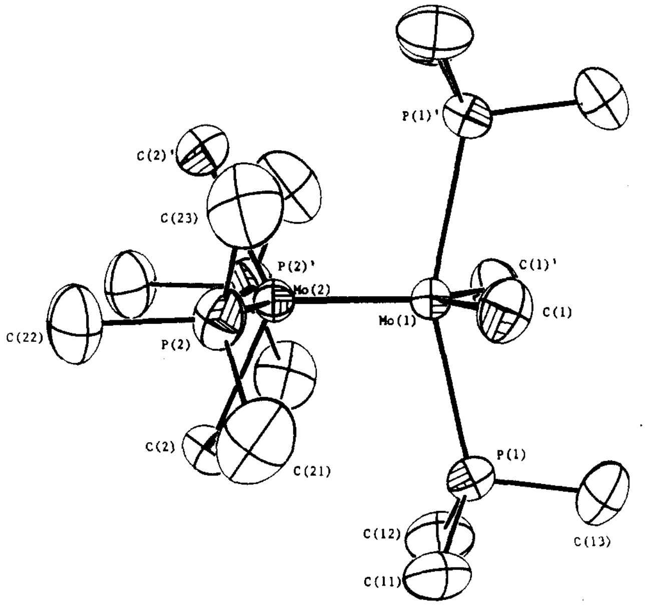

Figure 4. ORTEP drawing of the $Mo_2(CH_3)_4(PMe_3)_4$ (**2**) molecule. Atoms are represented by their ellipsoids at the 50% probability level.

3 react wih CF_3CO_2H and alcohols to give $Mo_2(O_2CCF_3)_4(PR_3)_2$ and $Mo_2(OR)_4(PR_3)_4$, respectively.

Structural Results. $Mo_2Cl_3(CH_2C_6H_5)(PMe_3)_4$. There is one molecule in the amounts of residual resides on a general position. An ORTEP drawing and numbering scheme of the molecule are shown in Figure 3. The Mo_2^{4+} core contains a quadruple bond [2.1382 (3) Å] between the metal center. In addition to the metal-metal bond, Mo(1) is bonded to Cl(1), P(1), P(2), and C(13) while Mo(2) is bonded to Cl(3), Cl(4), P(3), and P(4). This $Mo_2Cl_3P_4C$ core has idealized C_s symmetry. For the entire molecule to possess idealized C_s symmetry, the atoms Mo(1), Mo(2), C(13), C(14), and C(17) among others would need to lie in the mirror plane. This is not the case, as evidenced by the Mo(2)–Mo(1)–C(13)–C(14) torsion angle of −148.1 (2)°. Atoms C(14) and C(17) are removed from this mirror plane. To compensate for this twist, C(15) is forced up between the two trimethylphosphine groups and results in torsion angles of −70.7 (4) and 111.4 (3)° for Mo(1)–C(13)–C(14)–C(15) and Mo(1)–C(13)–C(14)–C(19), respectively. This results in a crystal that is composed of enantiomorphic pairs. As previously discussed, the ^1H NMR spectrum indicates that either the benzyl group is symmetrically oriented or the chiral conformations interconvert rapidly on the NMR time scale in solution. The chirality in the crystal could be the result of intermolecular forces alone.

The Mo(1)–C(13)–C(14) angle of 118.4 (2)° and the twist of the benzyl ligand preclude any ring π-donation to the σ^*_{Mo-Mo} orbital through the axial site.[7] The benzyl ligand is purely a σ-donor. The steric bulk of the benzyl ligand may contribute to the lengthening (0.026 Å) of the Mo(1)–P bond distances over the Mo(2)–P distances and to the lengthening (0.0165 Å) of the Mo(1)–Cl(1) bond distance over the Mo(2)–Cl distances.

$Mo_2(CH_3)_4(PR_3)_4$. In compounds **2** and **3**, the $Mo_2C_4P_4$ core adopts a D_{2d} idealized geometry. Each molybdenum center is bonded to another molybdenum, two methyl ligands, and two phosphine ligands where the non-metal ligands adopt a trans configuration.

The asymmetric unit for **2** contains half of one molecule. The ORTEP drawing and numbering scheme of **2** are shown in Figure 4. The Mo(1)–Mo(2) bond distance is 2.1489 (4) Å, and the bond is coincident with a crystallographic 2-fold axis. The Mo(1)–C(1) and Mo(2)–C(2) bond distances [2.248 (4) and 2.241 (3) Å] are consistent with the others found in Table II. The average of these two distances is 0.194 Å shorter than in Andersen's "$Mo_2(CH_3)_4(PMe_3)_4$".[9]

The asymmetric unit for **3** contains half of each of two independent molecules. The two molecules are virtually identical, and the ORTEP drawing and numbering scheme of one are shown in Figure 5. The average Mo–Mo bond distance is 2.164 [1] Å. The phenyl substituents on the PMe_2Ph ligand point out away from the molybdenum center, and the P–C axis is virtually parallel to the Mo–Mo axis. The other two methyl carbons are situated over the Mo–Mo axis.

The comparison of bond lengths and Mo radii for the $Mo_2Cl_4(PR_3)_4$ and $Mo_2(CH_3)_4(PR_3)_4$ species is quite interesting. In general, the Mo–Mo bond distance increases, the Mo–P bond distances decrease, and the calculated Mo radius increases in going from $Mo_2Cl_4(PR_3)_4$ to $Mo_2Me_4(PR_3)_4$. The increase in the calculated Mo radius indicates that the Mo_2^{4+} core becomes more

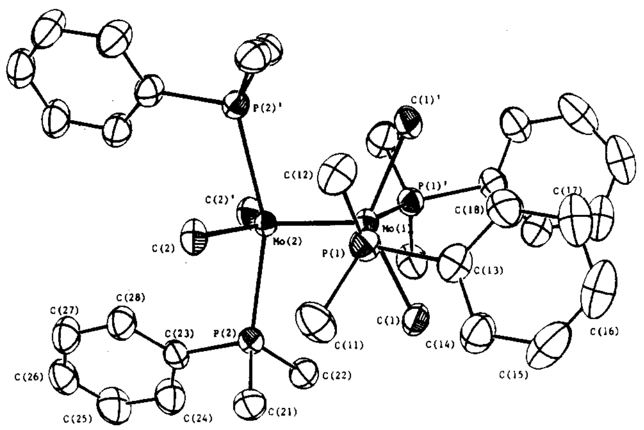

Figure 5. ORTEP drawing of the $Mo_2(CH_3)_4(PMe_2Ph)_4$ (**3**) molecule. Atoms are represented by their ellipsoids at the 50% probability level.

electron rich. The Mo–P bond distance presumably decreases because more Mo → P π bonding occurs. Both π and δ orbitals of the Mo–Mo bond could do this, thus lengthening the Mo–Mo bond.

Concluding Remarks

Synthesis of **1** revealed the ability of a Grignard reagent to act as either an alkylating or a halogenating agent. Synthesis of pure $Mo_2(CH_3)_4(PR_3)_4$ complexes, which are free of all halogen-containing contaminants, requires the use of $(CH_3)_2Mg$ prepared from $(CH_3)_2Hg$ in these systems. The structural investigations of **2** and **3** coupled with ^1H NMR evidence suggest that the material originally used to obtain the structure of **2** was actually a mixture of $Mo_2Cl_4(PMe_3)_4$ and $Mo_2(CH_3)_4(PMe_3)_4$. The Mo–C distances in Mo_2^{4+} core dimers are consistently 2.25 ± 0.02 Å. The Mo radius for $Mo_2(CH_3)_4(PR_3)_4$ is 0.05 Å larger than that of $Mo_2Cl_4(PR_3)_4$ species and indicates a more electron-rich Mo_2^{4+} core for alkyl-containing compounds.

Acknowledgment. We thank the National Science Foundation for financial support.

Supplementary Material Available: Tables for compounds **1**–**3** of all bond distances and angles, thermal parameters, and hydrogen coordinates and an ORTEP drawing of the second molecule of **3** (20 pages); tables of observed and calculated structure factors for **1**–**3** (57 pages). Ordering information is given on any current masthead page.

Contribution from the Chemistry Department, The Ohio State University, Columbus, Ohio 43210,
and Department of Chemistry, University of Warwick, Coventry CV4 7AL, England

Transition-Metal Complexes of Superstructured Cyclidene Macrobicycles: Structural Features and Their Chemical Consequences. 3.[1] Cyclidenes with Long Polymethylene Bridges

Nathaniel W. Alcock,*,† Peter A. Padolik, Graham A. Pike, Masaaki Kojima, Colin J. Cairns,
and Daryle H. Busch*,‡

Received November 28, 1989

The syntheses and X-ray structure determinations are reported for lacunar cyclidene complexes bridged by $-(CH_2)_9-$ (**9**) and $-(CH_2)_{10}-$ (**10**) chains. Correlation of these results with those for $-(CH_2)_8-$ and $-(CH_2)_{12}-$ bridges show how the transformations from the flat cavity increasing in width from $-(CH_2)_3-$ through $-(CH_2)_8-$ to the tall narrow cavity for $-(CH_2)_{12}-$ takes place through graduated conformational changes at the nitrogen atoms to which the bridging groups are attached. These changes can also be observed in ^{13}C NMR spectra, demonstrating that conformations are present in solution similar to those found in the solid state. Correlation of ^{13}C chemical shift with chain length over the range $-(CH_2)_n-$ (n = 3–10, 12) shows that some resonances are strongly influenced by cavity width. Other resonances show a small-scale alternation between n-odd and n-even, associated with the distortions required in bridges formed from even-membered chains. Crystal data: $C_{29}H_{50}N_6P_2F_{12}Ni.C_3H_6O$ (**9**), triclinic, $P\bar{1}$, a = 11.298 (6) Å, b = 13.615 (9) Å, c = 14.608 (10) Å, α = 75.48 (5)°, β = 73.32 (5)°, γ = 73.56 (5)°, Z = 2; $C_{30}H_{52}N_6P_2F_{12}Ni.C_2H_3N$ (**10**), orthorhombic, $P2_12_12_1$, a = 10.221 (4) Å, b = 13.723 (11) Å, c = 29.255 (16) Å, Z = 4.

Introduction

Previous studies in these laboratories[2] have established that the O_2 affinities of the lacunar cyclidenes (Figure 1) are strongly dependent on the shape and size of the molecular voids within which the dioxygen binds and that these are controlled by the nature of the substituents R^1–R^3. In a systematic study of this control, we examined the structures of the cyclidenes with polymethylene bridges $-(CH_2)_n-$, with n = 3–8 and 12.[1] The main trend in this series involves a linear increase in the cavity width as n goes from 3 to 8, culminating in one of the widest and flattest cavities yet identified (Figure 2a).

In remarkable contrast, in the cyclidene with a $-(CH_2)_{12}-$ bridge, the void is both narrow and extremely tall (Figure 2b). This difference does not merely result from the flexibility of the longer chain giving it the opportunity to stretch further and double back on itself. A substantial alteration has also taken place in the primary cyclidene unit. Rotation about the C–N bond of the nitrogen to which the bridge is attached is restricted by its partial double-bond character. In the absence of steric constraints, the substituents at this nitrogen (here the CH_3 and $-(CH_2)_n-$ chain) are oriented so that one group points directly away from the metal ion.[3,4] The bridge can take up either orientation, leading to the isomers described as "lid-on" and "lid-off" (Figure 3a,b).[3] The change from a $-(CH_2)_8-$ chain to a $-(CH_2)_{12}-$ chain involves the conversion from the lid-off to the lid-on form (compare the positions of C17 and C26 in Figure 2a with those of C11 and C11a in Figure 2b). This is potentially of particular significance in

---

* To whom correspondence should be addressed.
† University of Warwick.
‡ Department of Chemistry, The University of Kansas, Lawrence, KS 66045-0046.

(1) Part 2: Alcock, N. W.; Lin, W.-K.; Cairns, C.; Pike, G. A.; Busch, D. H. *J. Am. Chem. Soc.* **1989**, *111*, 6630.

(2) For a summary, see: Busch, D. H. In *Oxygen Complexes and Oxygen Activation by Transition Metals*; Martell, A. E., Sawyer, D. T., Eds.; Plenum Publishing Corp.: New York, 1988.

(3) Herron, N.; Nosco, D. L.; Busch, D. H. *Inorg. Chem.* **1983**, *22*, 2970.

(4) Alcock, N. W.; Cairns, C.; Jircitano, A. J.; Nosco, D. L.; Busch, D. H. *Acta Crystallogr., Sect. C* **1987**, *C43*, 2069.

0020-1669/90/1329-2599$02.50/0